IOP Publishing New J. Phys. 26 (2024) 093028 https://doi.org/10.1088/1367-2630/ad78f9

New Journal of Physics
The open access journal at the forefront of physics

Deutsche Physikalische Gesellschaft DPG
IOP Institute of Physics

Published in partnership with: Deutsche Physikalische Gesellschaft and the Institute of Physics

OPEN ACCESS

RECEIVED
23 April 2024

REVISED
6 September 2024

ACCEPTED FOR PUBLICATION
10 September 2024

PUBLISHED
19 September 2024

PAPER

Higher-order topological phase with subsystem symmetries

Yizhi You

Department of Physics, Northeastern University, Boston, MA 02115, United States of America

E-mail: y.you@northeastern.com

Keywords: subsystem symmetry, higher order symmetry protected topological phase, fracton, Lieb–Schultz–Mattis (LSM) theorem

Abstract

A wide variety of higher-order symmetry-protected topological phases (HOSPT) with gapless corners or hinges have been proposed as descendants of topological crystalline insulators protected by spatial symmetry. In this work, we address a new class of higher-order topological states that do not require crystalline symmetries but instead rely on subsystem symmetry for protection. We propose several strongly interacting models with gapless hinges or corners based on a *decorated hinge-wall condensate* picture. The hinge-wall, which appears as the defect configuration of a Z_2 paramagnet, is decorated with a lower-dimensional SPT state. Such a unique hinge-wall decoration structure leads to gapped surfaces separated by gapless hinges. The non-trivial nature of the hinge modes can be captured by a $1+1$D conformal field theory with a Wess–Zumino–Witten term. Moreover, we establish a no-go theorem to demonstrate the ungappable nature of the hinges by making a connection between the generalized Lieb–Schultz–Mattis theorem and the boundary anomaly of the HOSPT state. This universal correspondence engenders a comprehensive criterion to determine the existence of HOSPT under certain symmetries, regardless of the microscopic Hamiltonian.

1. Introduction

Quantum many-body systems prompt exotic phases of matter enriched by strong interactions and quantum entanglement. Tremendous effort has been made toward the classification and characterization of topological materials along with their bosonic descendants in the presence of internal and crystalline symmetries [1–13]. In addition to fully dispersive boundary modes, topological crystalline phases admit gapped edges or surfaces with protected gapless modes at high-symmetry corners or hinges. Exemplifying a much richer bulk-boundary correspondence, this phenomenology is now termed higher-order symmetry-protected topological phase (HOSPT) [14–18]. Beyond the non-interacting higher-order topological insulators and superconductors triggered by non-trivial band topology, a variety of boson (or interacting fermion) candidates for HOSPT with gapless corners or anomalous hinge states have appeared [19–22]. Apart from the mathematical characterization, the physical manifestations and material fabrications of HOSPT have appeared on a variety of platforms [23–25]. Moreover, there is increasingly compelling evidence to show that some higher-order topological superconductor corners can support exotic fractionalized quasi-particles including parafermions or projective Ising anyons [26, 27], providing new architectures for quantum information processing and quantum computation. At this stage, most examples of higher-order topology require crystalline symmetries. Due to the restriction of crystalline symmetry, the gapless corner or hinge modes are distributed in a spatially symmetric way. In the absence of spatial symmetry, one can typically hybridize and remove the spatially separated corner (hinge) modes through an edge (surface) phase transition without the bulk gap closing. It remains unclear whether a HOSPT state exists beyond crystalline symmetry protection [28].

In this work, we address HOSPT phases without crystalline symmetries, which instead rely on subsystem symmetry for protection [29–33]. In D spatial dimensions, subsystem symmetry consists of independent symmetry operations acting on a set of d-dimensional subsystems where $0 < d < D$. In $D = 3$, the subsystems can be lines ($d = 1$), planes ($d = 2$), or fractals [34–38]. The corresponding subsystem symmetry generates a

quantum number that is conserved separately on each sub-manifold, leading to interesting new possibilities for both symmetry-breaking [34] and symmetry-protected topological phases [35, 36, 39–42]. In [35, 36, 39, 40, 42], the authors introduced a zoology of subsystem-protected topological phases with gapless boundaries. Here, we propose a parallel 3D subsystem symmetric higher-order topological phase that supports gappable surfaces but gapless corners or hinges. Due to the subsystem symmetry that induces charge conservation on each 2D plane, the spatially separated gapless hinge or corner modes are robust against any symmetry-allowed perturbations. It is worth emphasizing that the subsystem symmetric HOSPT is an interaction-enabled higher-order topological phase. These nontrivial phases require putative strong interactions for their existence, and in the cases we consider, the free-fermion classification yields only a trivial phase.

To be more explicit, the general construction of a subsystem-symmetric HOSPT state depends on a decorated hinge-wall picture. As demonstrated in [41, 43–48], gauging a subsystem symmetric matter field leads to the fracton topological order with a cage-net (or membrane-cage-net) structure. By decorating such a membrane-cage-net structure with a nontrivial lower-dimensional SPT state, the hinge (corner) carries a fractional quantum number or symmetry anomaly, thus engendering a symmetry-enforced gapless hinge (corner). This construction, which we will present in the rest of the paper, is illuminating because it allows for a direct field-theoretic connection between subsystem HOSPT and symmetry-enriched Fracton gauge theories [46, 49].

Besides subsystem-symmetric HOSPT states from exactly solvable models, we also propose a general criterion for the existence of some particular subsystem-symmetric HOSPT phases by making a connection between the generalized Lieb–Schultz–Mattis (LSM) theorem and the boundary anomaly of a 3D HOSPT phase. Specifically, for a 3D HOSPT state protected by subsystem symmetry (G^{sub}) and global on-site symmetry (S), its symmetric boundary theory can be mapped into a 2D lattice model with subsystem symmetry (G^{sub}). Additionally, the lattice symmetry of such a 2D system acts in a similar way as the on-site symmetry (S) at the boundary of the HOSPT. This mapping between on-site symmetry at the boundary of a 3D HOSPT and lattice symmetry in 2D lattice models allows us to determine the possibility of a featureless gapped boundary. In particular, for 2D lattice models with subsystem symmetry [50], there is a general LSM theorem [51, 52] excluding the possibility of a featureless gapped phase hosting a unique ground state compatible with lattice and subsystem symmetry. The absence of such a featureless gapped phase in 2D implies that the 3D HOSPT boundary, with on-site symmetry S playing a role akin to the 2D lattice symmetry, does not admit a trivially gapped boundary (including the hinge) in the presence of on-site symmetry S and subsystem symmetry G^{sub}. Consequently, such an ungappable boundary with anomalous symmetry must be accompanied by a nontrivial bulk with higher-order topology. Based on such a well-established LSM theorem [53–59], one can readily determine the existence of HOSPT via its boundary actions even in the absence of any concrete Hamiltonian. As the LSM theorem is universal for any strongly interacting systems, the corresponding ungappable condition for the HOSPT boundary always applies, regardless of the microscopic Hamiltonian.

2. 3D HOSPT with protected corner mode

To start with, we first reboot our brains by examining a simple exactly solvable model on a cubic lattice. This model displays a HOSPT with a Majorana corner mode protected by subsystem fermion parity symmetry. Since our main tool is the study of exactly solvable model Hamiltonians, fermions introduce a new technical challenge: a fermion parity subsystem symmetry requires interactions that are at least quartic in the fermion operators. The resulting Hamiltonians are generally not solvable unless the interaction terms treat non-overlapping sets of fermions—and are necessarily not in the same symmetry class as any non-interacting topological phases of fermions. This also implies that the HOSPT protected by subsystem symmetry is unique in strongly interacting systems without any band-fermion analogy. Here, we will provide one example, constructing a 3D charge 4e superconductivity model with subsystem fermion parity symmetry on each $i-j$ plane.

We begin with four fermions on each site of the cubic lattice as shown in figure 1. One can decompose the four fermions on each site into eight Majorana operators labeled as $\eta_1, \ldots, \eta_8$. On each cube, there are several Majorana quartet interactions among the eight Majoranas residing at the cube corners. Of the eight fermions on each site, each participates in the cluster interaction term in one of the eight nearby cubes, ensuring that all interactions commute.

To describe the interaction terms, we label the eight Majoranas as shown in figure 1. Each cube cluster containing eight Majorana fermions is coupled via Fidkowski–Kitaev [60, 61] type interactions. Specifically,

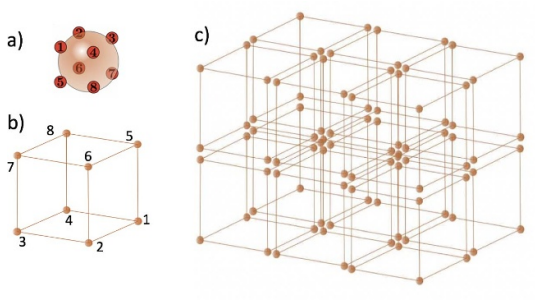

Figure 1. (a) Each site has eight Majoranas $\eta_1, \ldots, \eta_8$. (b), (c) The eight Majoranas living at the corner of each cube are projected into a unique ground state preserving coplanar fermion parity symmetry.

we first add a 4-Majorana interaction among the Majoranas on the top and bottom surfaces as follows:

$$H_1 = \eta_5\eta_6\eta_7\eta_8 + \eta_1\eta_2\eta_3\eta_4. \tag{1}$$

Ground states of H_1 can be described via the complex fermions,

$$\begin{aligned} \Psi_\uparrow &= \eta_5 + i\eta_6, \Psi_\downarrow = \eta_7 + i\eta_8 \\ \Psi'_\uparrow &= \eta_1 + i\eta_2, \Psi'_\downarrow = \eta_3 + i\eta_4. \end{aligned} \tag{2}$$

In these variables, the Hamiltonian H_1 becomes,

$$H_1 = (n_\Psi - 1)^2 + (n_{\Psi'} - 1)^2. \tag{3}$$

Thus H_1 favors the odd fermion parity state for both Ψ and Ψ'. This allow us to map the ground state subspace of H_1 into two spin $1/2$ degrees of freedom per cube:

$$\vec{n}_i = \Psi^\dagger \vec{\sigma}_i \Psi, \vec{m}_i = \Psi'^\dagger \vec{\sigma}_i \Psi'. \tag{4}$$

In terms of these spin degrees of freedom, the second interaction on the cube cluster is,

$$\begin{aligned} H_2 &= -m_x n_x - m_y n_y \\ &= (\eta_5\eta_6 - \eta_7\eta_8)(\eta_1\eta_2 - \eta_3\eta_4) \\ &\quad + (\eta_5\eta_8 - \eta_6\eta_7)(\eta_1\eta_4 - \eta_2\eta_3). \end{aligned} \tag{5}$$

Such an XY interaction projects the two spins in each cube cluster into an SU(2) singlet, yielding a unique ground state. With this cluster interaction on each cube, as shown in figure 1, the many-body Hamiltonian is fully gapped with a unique ground state in the bulk.

What are the symmetries of this model? Due to the quartet nature of the Majorana interaction, our Hamiltonian conserves the fermion parity of each $x-y$, $y-z$, and $x-z$ plane separately. This subsystem fermion parity symmetry implies that any fermion-bilinear interaction between sites is prohibited, so the leading-order inter-site couplings are the quartet interactions.

In the presence of a boundary, each surface (or hinge) site contains four (or two) unpaired Majoranas, which can be gapped out via onsite Majorana hybridization. When it comes to the corner, the corner site carries seven free Majorana zero modes, which cannot be gapped out via onsite hybridization. Additionally, due to the subsystem fermion-parity symmetry, one cannot hybridize or gap out the Majorana zero modes from different corners via surface/hinge phase transitions (while keeping the bulk gap), as such coupling always breaks the fermion parity on specific $i-j$ planes. Thus, the Majorana zero mode on each corner is robust under subsystem fermion-parity symmetry.

Several earlier pieces of literature [14, 15, 62] propose a class of third-order topological insulators/superconductors in 3D with corner zero modes. However, these corner modes can be annihilated via hinge/surface phase transitions without closing the bulk gap. Accordingly, these models are not intrinsically topological as the existence of the corner mode is not connected to the bulk physics. To illustrate this subtlety, we note that since there are *three* hinges that terminate at a corner, one can always, in principle, decorate the hinges with nontrivial 1D SPT chains on all hinges to cancel out the corner modes. Consequently, there is no 'intrinsic fermionic topological octupole insulator' with robust corner modes protected by cubic symmetry [63, 64]. However, with the additional subsystem fermion parity symmetry, a

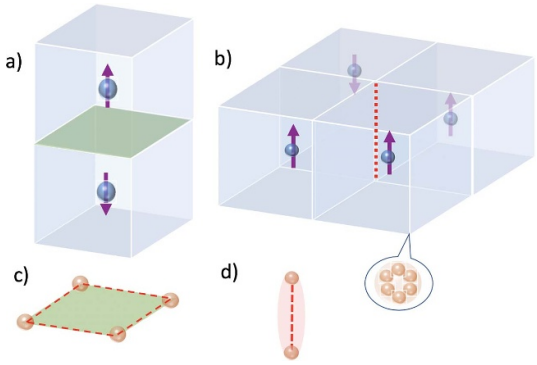

Figure 2. (a) The σ^z domain wall on the $x-y$ plane. (b) The hinge defect along the z-link. (c) Each $x-y$ domain wall is decorated with a 2D HOSPT with protected spin 1/2 corner mode(red dot). (d) Each z-hinge defect is decorated with SU(2) singlet.

fermionic HOSPT with gapless corner modes becomes a reality, as the subsystem symmetry strictly constrains the interactions. It is worth mentioning that our subsystem fermion parity symmetric HOSPT does not have a non-interacting counterpart, as any fermion hopping term would break subsystem fermion parity in any case. Thus, the subsystem symmetric HOSPT is a unique feature in strongly interacting systems.

3. 3D subsystem HOSPT with gapless hinges

Thus far, we have developed a third-order topological phase with gapless corner modes protected by subsystem symmetry. Specifically, such a class of subsystem symmetric HOSPT always requires putative strong interactions without a free-fermion counterpart. We will now proceed to formulate a second-order topological phase with gapless hinges protected by subsystem symmetries. In particular, we are interested in cases where the many-body system carries both subsystem symmetry G^{sub} and global symmetry S. If such a state manifests a higher-order topological phase, the global symmetry defect S at the hinge carries a fractional quantum number of G^{sub}, making the hinge ungappable. Moreover, the surface and hinge theory of such an HOSPT can be mapped into a lower-dimensional lattice system with the same subsystem symmetry (G^{sub}). At the same time, the lattice symmetry acts in a similar way as the on-site symmetry (S) at the boundary of HOSPT. Such a mapping between on-site symmetry at the boundary of a 3D HOSPT and lattice symmetry in 2D lattice models allows us to determine the possibility of a featureless gapped boundary based on the LSM theorem. This noteworthy mapping establishes a general criterion for the existence of the higher-order topological phase under $G^{\text{sub}} \times S$ symmetry.

3.1. Decorated hinge-wall model

To begin, let us look into a spin model on a BCC lattice as shown in figure 2. The cube center contains a single Ising spin σ (blue dot), while the cube corner carries six spin-1/2 degrees of freedom labeled as τ (red dots). The spin σ living at the cube center is placed into a Z_2 paramagnetic phase,

$$H_\sigma = -\sum_i \sigma_i^x. \tag{6}$$

This Hamiltonian has a global Z_2 symmetry generated by σ^x. In the paramagnetic phase, the σ spins are polarized in the x-direction. If we choose the σ^z basis, the ground state wave function is a coherent superposition of all domain wall membrane configurations on the cubic lattice, which separate the regions between $\sigma^z = 1$ and $\sigma^z = -1$.

The interaction among the τ spins from the cube corners depends on the adjacent σ spin structure. In particular, if the two σ^z spins form a domain wall on the $x-y$ plane, as $\sigma^z(r+\frac{e_z}{2})\sigma^z(r-\frac{e_z}{2}) = -1$ shown in figure 2, we decorate such a domain wall plaquette on the $x-y$ plane by creating a four-spin entangled pair $|\psi\rangle_{r+e_z} = |0101\rangle + |1010\rangle$ among the four τ spins on the corners of the domain wall plaquette. Such decoration can be expressed in terms of the projection Hamiltonian

$$H^1_{\sigma,\tau} = \left(1+\sigma^z\left(r+\frac{e_z}{2}\right)\sigma^z\left(r-\frac{e_z}{2}\right)\right)|\psi_{r+e_z}\rangle\langle\psi_{r+e_z}|. \tag{7}$$

The state $|\psi_{r+e_z}\rangle$ refers to the four spins entangled on the corners of the domain wall plaquette. When the σ^z spins above and beneath form a domain wall, the four τ spins from the plaquette corners are projected into

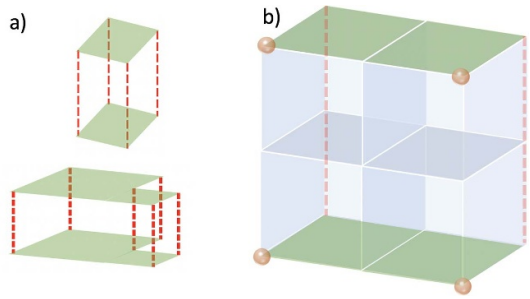

Figure 3. (a) The ground state is a superposition of all possible domain wall configurations of σ^z. Here, the green plaquette illustrates the domain wall on the $x-y$ plane, while the red dashed line represents the z-hinge as an intersection line between the domain walls of the xz and yz planes. The domain wall on the $x-y$ plane is decorated with a 2D HOSPT featuring a spin-1/2 corner mode, while the z-hinge carries an AKLT chain along the z-direction. In image (b), when the green domain wall on the $x-y$ plane meets the side boundary, the corner hosts an unpaired spin-1/2.

the ψ state. When it comes to the corner of the domain wall on the $x-y$ plane, as shown in figure 2, the corner site contains an odd number of unpaired spin-1/2 zero modes protected by $\mathcal{T}$. Meanwhile, all other sites contain an even number of spin-1/2, which can be gapped out by pairing them into an onsite singlet. Based on this observation, each domain wall on the $x-y$ plane is embellished with a 2D HOSPT with protected spin-1/2 corner modes [26].

In addition, when the four σ spins adjacent to each z-hinge contain an odd number of $\sigma^z=-1$ as shown in figure 2, we decorate the z-hinge by creating a two-spin entangled pair $|\phi\rangle_r=|01\rangle-|10\rangle$ between the two τ spins at the end of the z-link. Such decoration can be expressed in terms of the projection Hamiltonian

$$H^2_{\sigma,\tau}=\left(1+\sigma^z\left(r-\frac{e_x+e_y}{2}\right)\sigma^z\left(r-\frac{e_x-e_y}{2}\right)\sigma^z\left(r+\frac{e_x+e_y}{2}\right)\sigma^z\left(r+\frac{e_x-e_y}{2}\right)\right)|\phi_r\rangle\langle\phi_r|. \tag{8}$$

When the four σ spins adjacent to the hinge have an odd number of spin-down states, the two τ spins between the hinge are projected into an SU(2) singlet. Such a 'hinge defect' can be regarded as the intersection line between two σ domain walls from the yz and xz planes. The interaction in equation (8) embellishes each 'z-hinge defect' with an AKLT chain along the z-row. This AKLT chain, decorated on the z-hinge, preserves $U^{\text{sub}}(1)$ and global $\mathcal{T}$ symmetry as defined in equation (9). As the interaction between τ spins only occurs along the z-hinge, the S_z quantum number on each xz and yz plane is still preserved. Since the z-hinge defect carries an AKLT chain, the open end of the z-hinge defect contains a spin-1/2 zero mode.

Apart from the Z_2 symmetry for σ, this Hamiltonian possesses a global time-reversal symmetry $\mathcal{T}$ for τ that flips each spin, and a subsystem $U(1)$ symmetry that preserves the τ^z number on each xz and yz plane

$$\begin{aligned}&\mathcal{T}=\mathcal{K}i\tau^y,\\&U^{\text{sub}}(1):\prod_{j\in P_{i-z}}e^{i\frac{\theta}{2}\tau^z_j}.\end{aligned} \tag{9}$$

The subsystem $U(1)$ symmetry acts only on the six τ spins inside each unit cell in each yz or xz plane and rotates the τ spin around the S_z axis. Hence, subsystem $U(1)$ symmetry preserves the total S_z charge of τ along any yz and xz plane, and forbids spin-bilinear coupling between the S_x, S_y channels on x (or y) links. Furthermore, the global $\mathcal{T}$ symmetry forbids terms in the Hamiltonian that would polarize the spins.

The Hamiltonian we construct here has a simple ground state wave function. As the σ spin located at the cube center is in the Z_2 paramagnetic phase, its ground state can be expressed as a superposition of all closed domain wall configurations in the bulk. Meanwhile, due to the τ spin decoration in equations (7) and (8), the domain wall on the $x-y$ plane contains a spinon mode at the rough corner of the domain wall, while the z-hinge defect is decorated with an AKLT chain. The z-hinge defect is essentially the domain wall intersection line between the xz and yz planes. Any open end of the z-hinge defect connects to the domain wall corner on the xy plane, as shown in figure 3. This connection results from the closed domain wall configuration in the bulk, and the connecting point between the z-hinge end and the $x-y$ domain wall corner is merely the intersection point among three domain wall planes from the xy, yz, and xz directions. As a result, the ground state can be viewed as a hinge-wall condensate, with each z-hinge connecting to a domain wall corner from the xy plane. The spin-1/2 zero mode residing at the corner of the $x-y$ domain wall can hybridize with the dangling spin-1/2 at the end of the z-hinge defect. Consequently, the hinge-wall condensation gives rise to a gapped state in the bulk.

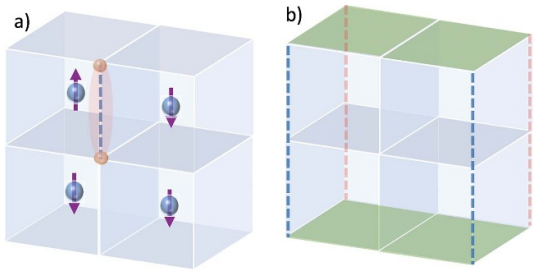

Figure 4. (a) The z-domain wall line on the side face between two anti-parallel σ^z spins is decorated with a spin singlet formed by τ. (b) The $x-y$ domain wall corner meeting the side surface is connected to the surface domain wall line along the z-direction. Since the z-domain wall line on the side face is decorated with an AKLT chain, the connecting point can be fully gapped.

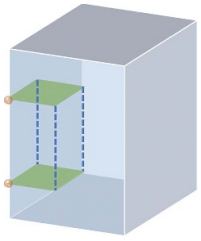

Figure 5. When the corner of the $x-y$ domain wall meets the hinge, a free spin-1/2 zero mode (red dot) appears. The proliferation of such domain walls at the 1D hinge, each carrying a spin-1/2 mode, leads to a gapless hinge state.

When it comes to the surface, we first focus on the side faces on yz and xz planes. As is illustrated in figure 3, the corner of the $x-y$ domain wall hitting at the side faces on yz (or xz) plane is no longer connected by a z-hinge. Such open $x-y$ domain wall corner at the boundary carries a free spin-1/2 zero mode. We now construct a symmetry-preserving surface perturbation that fully gap out the degree of freedom on the side faces

$$\begin{aligned} H_{x-\text{zsurface}} &= \left(1+\sigma^z\left(r-\frac{e_x}{2}\right)\sigma^z\left(r+\frac{e_x}{2}\right)\right)\ |\phi_r\rangle\langle\phi_r|, \\ H_{y-\text{zsurface}} &= \left(1+\sigma^z\left(r-\frac{e_y}{2}\right)\sigma^z\left(r+\frac{e_y}{2}\right)\right)\ |\phi_r\rangle\langle\phi_r|. \end{aligned} \tag{10}$$

The surface interaction decorates the z-directional domain wall line on each xz (yz) surface with an AKLT chain formed by τ spin. As the AKLT chain consists of inter-site dimer singlets between z-links, it preserves the $U^{\text{sub}}(1)$ on xz and yz planes as well as global $\mathcal{T}$ symmetry. The surface domain wall lines along the z-direction are connected by the corner of the $x-y$ domain wall that meets the boundary, as shown in figure 4. Such connecting points contain two spin-1/2 zero modes contributed by the $x-y$ domain wall corner and the z-directional surface domain wall end. By coupling these two spin-1/2 zero modes, the surface area is fully gapped.

We now consider the degrees of freedom on the z-hinge. Based on our bulk Hamiltonian, if there is a domain wall between $\sigma^z(r-\frac{e_z}{2})$ and $\sigma^z(r+\frac{e_z}{2})$ at the hinge, the domain wall point carries a spin-1/2 zero mode, as shown in figure 5. Such a point defect on the hinge can be regarded as the corner of the $x-y$ plane domain wall meeting the hinge. The global Z_2 symmetry for the σ spin ensures the fluctuation and proliferation of the domain wall at the hinge, while the $U^{\text{sub}}(1)$ and $\mathcal{T}$ protect the spin-1/2 zero mode (for τ spin) decorated within the domain wall on the z-hinge.

As the domain wall on the hinge carries a spinon degree of freedom, its condensate either breaks $U^{\text{sub}}(1)$ and $\mathcal{T}$ symmetry or results in a gapless state. Indeed, this gapless hinge mode is described by a $(1+1)D$ topological field theory with an $O(4)_1$ WZW term [65–68]

$$\begin{aligned} &\mathcal{L}_{\text{edge}} = \frac{1}{g}(\partial_\mu \vec{n})^2 + \frac{2\pi}{\Omega^3}\int_0^1 \mathrm{d}u\ \epsilon^{ijkl} n_i \partial_z n_j \partial_t n_k \partial_u n_l, \\ &\vec{n}(x,t,u=0) = (1,0,0,0), \quad \vec{n}(x,t,u=1) = \vec{n}(x,t) \\ &n_4 = \langle\sigma_z\rangle,\ n_1 = \langle\tau_x\sigma_z\rangle,\ n_2 = \langle\tau_y\sigma_z\rangle,\ n_3 = \langle\tau_z\sigma_z\rangle. \end{aligned} \tag{11}$$

The $O(4)$ WZW term implies that the domain wall of σ_z carries a $(0+1)D$ $O(3)_1$ WZW term which exactly represents a spin-1/2 degree of freedom. The global Z_2 and $\mathcal{T}$ symmetry act on the $O(4)$ vector boson as,

$$\begin{aligned} &Z_2 : \vec{n}(x,t) \to -\vec{n}(x,t); \\ &\mathcal{T} : (n_1, n_2, n_3) \to (-n_1, -n_2, -n_3). \end{aligned} \tag{12}$$

The subsystem $U(1)$ symmetry rotates the hinge spin along the τ^z axis as,

$$\begin{aligned} &e^{i\theta} = n_1 + i n_2, \\ &U^{\text{sub}}(1) : e^{i\theta} \to e^{i\theta+\alpha}. \end{aligned} \tag{13}$$

Clearly, the $O(4)$ WZW theory on the hinge is invariant under $U^{\text{sub}}(1) \times \mathcal{T} \times Z_2$. These symmetries prevent polarization of any components in the $O(4)$ vector, and the non-vanishing $O(4)_1$ WZW term consistently results in a gapless hinge, similar to a $(1+1)D$ $SU(2)_1$ CFT [66, 69].

In this example, we are dealing with continuous subsystem symmetry (like $U(1)$), so the anomaly can be easily clarified using the flux insertion argument. For considerations of discrete subsystem and global symmetries in HOSPTs, one can apply the Nayak–Else argument [28, 70] by introducing subsystem symmetry defects. By analyzing the symmetry representation of the defect on the hinge, one can demonstrate that the symmetry action across the defect is non-onsite, creating an obstruction to implementing such symmetry in lower-dimensional lattice models.

3.2. LSM theorem perspective

Our previous analysis only demonstrates a specific way to gap out the side faces, separated by a gapless z-hinge, under symmetry protection. However, unlike the justification we adopted for conventional SPT boundaries, the stability of each symmetry protected gapless hinge does not guarantee nontrivial bulk topology. Despite the fact that the spatially separated hinges are stably gapless individually, they might still be hybridized and gapped through surface phase transitions (without gap closing in the bulk). It remains unclear whether the hinge is ungappable or anomalous under any symmetry-allowed surface reconstruction. To demonstrate the necessity of a gapless hinge, we implement an LSM theorem argument here to elucidate the ungappable nature of the hinge state.

The connection between the ungappable boundary of an SPT surface and the absence of a featureless gapped insulator can be traced back to references such as [53–58]. The generalized LSM theorem states that some D-dimensional quantum many-body systems with internal symmetry G and lattice symmetry S do not allow a featureless gapped phase with a unique ground state invariant under $G \times S$. In parallel with such a lattice no-go theorem, an SPT boundary that is anomalous under G and onsite $\tilde{S}$ symmetry does not support a featureless gapped surface state without breaking $G \times \tilde{S}$. Under ultraviolet regularizations, the lattice symmetry S can be interpreted as an internal symmetry $\tilde{S}$, and the low-energy effective theory of the D-dimensional SPT boundary with $G \times \tilde{S}$ is equivalent to the $D-1$-dimensional lattice model with $G \times S$ symmetry. This mapping has led to fruitful results: As an SPT boundary with $G \times S$ symmetry does not permit a trivial gapped boundary, the corresponding lattice spin systems cannot hold a featureless gapped phase. Likewise, if a generalized LSM theorem implies the absence of a featureless gapped ground state, one can extrapolate that the surface theory from dual-mapping is anomalous and thus must rely on a nontrivial bulk state.

Here we first explicate that our surface theory on xz and yz planes with $U^{\text{sub}}(1) \times \mathcal{T} \times Z_2$ symmetry can be mapped into a 2D lattice model with $U^{\text{sub}}(1) \times \mathcal{T}$ and translation symmetry T_z. In our current settings, each $x-y$ domain wall corner hitting at the xz side face carries a spin-1/2 degree of freedom. Such domain wall corner on the side face can be defined as,

$$\sigma^z\left(r - \frac{e_x + e_z}{2}\right)\sigma^z\left(r - \frac{e_x - e_z}{2}\right)\sigma^z\left(r + \frac{e_x + e_z}{2}\right)\sigma^z\left(r + \frac{e_x - e_z}{2}\right) = -1. \tag{14}$$

We are now about to map the surface theory into a 2D square lattice model with two (or an even number of) spin-1/2 degrees of freedom per site. We first define a valence plaquette state as shown in figure 6, where four spin-1/2s from the four corners of a plaquette are entangled as $|0101\rangle + |1010\rangle$. Such a valence plaquette state preserves the $U^{\text{sub}}(1) \times \mathcal{T}$ symmetry defined in equation (13). Based on such a valence plaquette configuration, which breaks lattice translation, one can map the plaquette order into a Z_2 variable.

$$Q(r) = \left(P(r + e_z/2) - P(r - e_z/2)\right), P \in 0, 1 \tag{15}$$

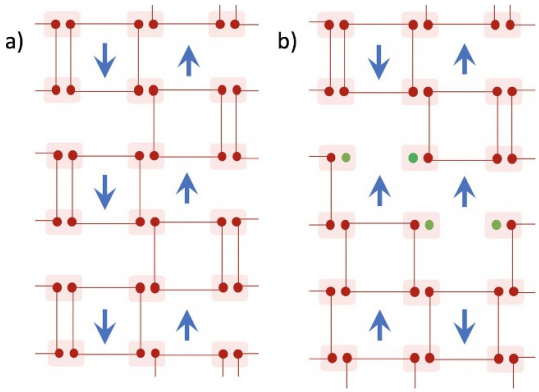

Figure 6. (a) Square lattice with two spin-1/2 per unit cell. The red square represents the valence plaquette state. The blue arrow characterizes the Z_2 variable of the plaquette order parameter Q. (b) When the plaquette order parameter Q exhibits a point defect, each defect carries an unpaired spin-1/2 (green dot).

where $P=1$ (or 0) corresponds to the valence plaquette occupancy (or vacancy) on each square. $Q(r)$ is thus a Z_2 variable characterizing the valence plaquette order. In particular, this plaquette order is odd under translation symmetry along the z-direction, so the unit cell is doubled

$$T_z : Q(r) \to Q(r+e_z) = -Q(r). \tag{16}$$

This symmetry action resembles the global Z_2 symmetry acting on the σ^z degree of freedom at the surface of the HOSPT. Furthermore, if the plaquette order exhibits a point defect, as

$$Q\left(r-\frac{e_x+2e_z}{2}\right)Q\left(r-\frac{e_x-2e_z}{2}\right)Q\left(r+\frac{e_x+2e_z}{2}\right)Q\left(r+\frac{e_x-2e_z}{2}\right)=-1. \tag{17}$$

This point defect carries a spin-1/2 zero mode due to the unpaired spinon surrounded by the plaquette. This defect structure is similar to that described in equation (14), where the corner defect of four adjacent Z_2 variables carries a spin-1/2 mode.

Based on these observations, we map the surface of the HOSPT into a 2D lattice model. The primary degree of freedom on both sides of the mapping involves a τ spin with $U^{\text{sub}}(1)\times\mathcal{T}$ symmetry. Additionally, the valence plaquette ordering in a 2D square lattice can be mapped into a Z_2 variable $Q(r)$, which is odd under discrete translation T_z. Similarly, the σ^z spin on the surface of the HOSPT is odd under global Z_2. On both sides of the mapping, the plaquette defect in equation (17) and the σ^z corner defect in equation (14) carry a spin-1/2 degree of freedom. Consequently, the effective theory of the 2D spin model with $U^{\text{sub}}(1)\times\mathcal{T}\times T_z$ on a square lattice is equivalent to the HOSPT surface with $U^{\text{sub}}(1)\times\mathcal{T}\times Z_2$ symmetry. A no-go theorem for a featureless gapped ground state on the square lattice can be extrapolated to the absence of a symmetry-invariant gapped HOSPT surface.

For a square lattice with two spins per unit cell, one can construct a featureless gapped ground state that preserves $U^{\text{sub}}(1)\times\mathcal{T}$ and translation symmetry T_z. To gain intuition, let us first interpret the Pauli spin operators in terms of hardcore bosons:

$$\tau^x+i\tau^y=a^\dagger, \tau^x-i\tau^y=a, \tau^z=a^\dagger a-1/2. \tag{18}$$

Each hardcore boson has a restricted onsite filling, $a^\dagger a=0,1$, and the states $|0\rangle$ and $|1\rangle=a^\dagger|0\rangle$ carry a $U(1)$ charge of $-1/2$ and $1/2$, respectively. The boson creation operator $a^\dagger$ creates an $S_z=1$ magnon excitation by changing $S_z\to S_z+1$.

In this language, the subsystem $U(1)$ symmetry becomes a phase rotation for the bosons on each z-row at the side face

$$U^{\text{sub}}(1) : a_j \to e^{i\theta}a_j,\ \ j\in\text{row}. \tag{19}$$

Additionally, $\mathcal{T}$ acts as a particle-hole symmetry for the hardcore bosons,

$$\mathcal{T} : |1\rangle\to|0\rangle, |0\rangle\to-|1\rangle \tag{20}$$

$$a\to-a^\dagger, a^\dagger\to-a. \tag{21}$$

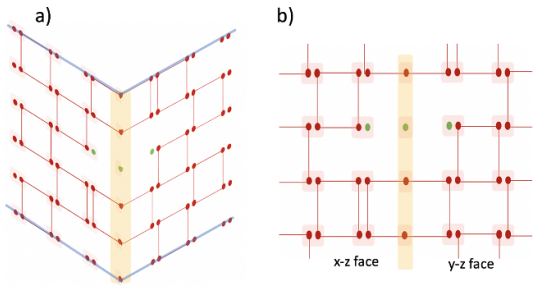

Figure 7. (a) The hinge(yellow shaded area) of the HOSPT can be mapped into a spin 1/2 chain with an odd number of spins per site. (b) projected view of the z-hinge connecting two surfaces.

For a $\mathcal{T}$ invariant ground state, the boson filling fraction is fixed as $\nu = 2(S_z + 1/2) = 1$ [71].

Constructing a featureless gapped ground state is straightforward. With two spin-1/2 per site, one can always pair the two spins per site into an onsite singlet, resulting in a unique gapped ground state that preserves the $U^{\text{sub}}(1) \times \mathcal{T}$ and translation symmetry. However, when it comes to a hinge, the Z_2 domain wall of σ^z carries an unpaired spin-1/2 on the hinge. Such a hinge structure can be mapped into a spin chain with an odd number of spin-1/2 per site, as shown in figure 7. The VBS order parameter plays the role of a Z_2 variable which is odd under translation T_z. Each VBS domain wall carries a spin-1/2 zero mode, so the effective theory of such a chain resembles the hinge of HOSPT.

Based on this observation, the xz and yz surfaces can be mapped into a square lattice model with two (or even) numbers of spin-1/2 per site. The hinge corresponds to a defect line along the z-direction with an odd number of spin-1/2 per site, as shown in figure 7. If the lattice system permits a featureless ground state with a finite gap in the presence of translation and $U^{\text{sub}}(1) \times \mathcal{T}$, a necessary condition requires that each row along the z-direction must carry an even number of spin-1/2 per site. To be more explicit, we first assume there is a short-range entangled ground state that is invariant under lattice translation and subsystem $U(1)$ symmetry on each z-row. Now we implement a 2π flux insertion on a specific z-row

$$U_{z,i} = \exp\left(\frac{2\pi i}{L_z} \sum_{r \in i\text{th row}} z\hat{n}_r\right). \tag{22}$$

Such a large gauge transformation creates a 2π flux for the ith row along the z-direction. Due to subsystem charge conservation, the global flux on each z-row is independent. For a featureless gapped ground state $|g\rangle$, such a large gauge transformation leaves the $|g\rangle$ state invariant. Meanwhile, as $|g\rangle$ is translation invariant under T_z, we can shift the ground state by one lattice spacing a. Combining these two operations together,

$$\begin{aligned} T_z U_{z,i}|g\rangle &= e^{i2\pi \sum_{r \in i\text{th row}} \hat{n}_r a/L_z} U_{z,i} T_z |g\rangle \\ &= e^{i2\pi \nu_i} U_{z,i} T_z |g\rangle. \end{aligned} \tag{23}$$

Here ν_i is the filling fraction of the spin-1/2 (hardcore boson) on the ith row. When a specific z-row has an odd number of spin-1/2 per site, we reach an obstruction that,

$$T_z U_{z,i}|g\rangle = -U_{z,i} T_z |g\rangle. \tag{24}$$

This contradicts the assumption that $|g\rangle$ is a unique ground state invariant under $U^{\text{sub}}(1)$ and translation. Thus, there is no featureless gapped ground state if there is a row with an odd number of spin-1/2 per site. In the absence of a hinge, each z-row has an integer filling fraction, so the side faces can be gapped. However, the hinge creates an extra row with a half-filling fraction, whose ground state is either gapless or symmetry-breaking.

4. Fermionic HOSPT with gapless hinge mode

Current interest in higher-order topology is primarily driven by the material realization of fermion band theories [5, 12, 14, 24, 72–74]. This raises the question of whether HOSPT protected by subsystem symmetry can be realized in interacting fermion systems. As we highlighted in previous discussions, the subsystem symmetric HOSPT states do not have non-interacting counterparts, as any fermion bilinear term inevitably breaks subsystem symmetry. Thus, most prominent constructions for fermion HOSPT cannot be readily translated to interacting systems, which require a fundamentally different approach. In the process, we will

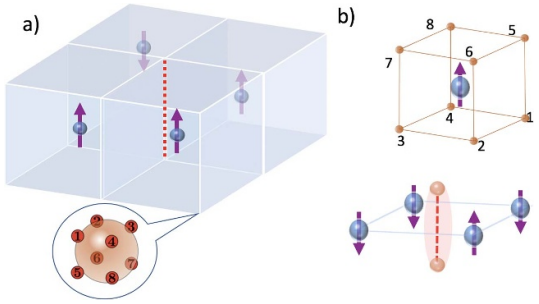

Figure 8. (a) The cube center contains an Ising spin, and the cube corner carries eight Majoranas. (b) The eight Majoranas at the corner of the cube are projected into a unique state if the center spin is polarized in the up direction. If the four σ spins adjacent to the z-hinge contain an odd number of $\sigma^z=-1$, we hybridize the two Majoranas $i\eta(r)\eta(r+e_z)$ between the z-link.

uncover an alternative route by implementing the decorated hinge-wall picture in fermion systems. This construction can be regarded as the fermionic version of the HOSPT we developed in section 3 by replacing the τ spins decorated on the hinge-wall with Majorana fermions.

To begin, let us examine a fermion model on a BCC lattice in figure 8. The cube center contains a single Ising spin σ (blue dot), while the cube corner carries eight Majoranas (red dots). The spin σ living at the cube center is placed into a Z_2 paramagnetic phase,

$$H_\sigma=-\sum_i \sigma_i^x. \tag{25}$$

Such Hamiltonian has a global Z_2 symmetry generated by σ^x. In the paramagnetic phase, the σ spins are polarized in the x-direction. If we choose the σ^z basis, the ground state wave function of such a paramagnet is a coherent superposition of all domain wall configurations on the cubic lattice. The interactions among the Majoranas from the cube corners depend on the adjacent σ spin structure. In particular, for each cube center with $\sigma^z=-1$, we project the eight Majoranas from the eight corners of each cube into a unique ground state in the same way as described in equations (1)–(5). As elucidated in section 2, such interaction preserves the subsystem fermion parity symmetry on both the xz and yz planes. Based on the discussion in section 2, this decoration structure embellishes the σ^z domain wall corner (the intersection point between three domain walls from the xy, xz, and yz planes) with a Majorana zero mode.

Meanwhile, when the four σ spins adjacent to each z-hinge contain an odd number of $\sigma^z=-1$ as shown in figure 8, we decorate the z-hinge by creating a two-Majorana entangled pair $i\eta(r)\eta(r+e_z)$ on the z-link. This 'hinge defect' can be regarded as the intersection line between two domain walls from the yz and xz planes. The Majorana hybridization embellishes each 'z-hinge defect' with a Kitaev chain, which still preserves subsystem fermion parity on the xz and yz planes. The open end of the z-hinge defect contains a free Majorana zero mode.

This Hamiltonian we construct here has a simple ground state wave function. As the σ spin living at the cube center is in the paramagnetic phase, its ground state can be expressed in terms of a superposition of all closed domain wall configurations in the bulk. Meanwhile, due to the Majorana decoration, the domain wall on each $x-y$ plane contains a Majorana corner mode, while the z-hinge defect is decorated with a Kitaev chain. As the z-hinge defect is nothing but the domain wall intersection line between the xz and yz planes, any open end of the z-hinge defect should be connected to the domain wall corner of the xy plane. As a result, the ground state can be viewed as a hinge-wall condensate with each z-hinge connecting a domain wall corner from the xy plane. The Majorana zero mode contributed from the corner of the $x-y$ domain wall can hybridize with the Majorana zero mode contributed from the end of the z-hinge defect. Subsequently, the decorated hinge-wall condensate generates a gapped phase with a unique ground state.

When it comes to the surface on the yz and xz planes, the corner of the $x-y$ domain wall hitting the side faces on the yz (or xz) plane is no longer connected by a z-hinge. Such an open $x-y$ domain wall corner at the boundary carries an unpaired Majorana zero mode. Following the procedure in section 3, we can construct symmetry-preserving surface perturbations which fully gap out the degree of freedom on the side faces. By decorating the z-directional domain wall line on each xz (yz) surface with a Kitaev chain, the side face is fully gapped.

We now consider the degrees of freedom on the z-hinge. Based on our construction, if there is a domain wall between $\sigma^z(r-\frac{e_z}{2})$ and $\sigma^z(r+\frac{e_z}{2})$ at the hinge, the domain wall point carries a Majorana zero mode. The global Z_2 symmetry for the σ spin guarantees the fluctuation and proliferation of domain walls, while the subsystem fermion parity protects the Majorana zero mode decorated inside.

Such hinge structure can be mapped into a 1D Majorana chain with an odd number of Majoranas per site. One can further define a bond order parameter,

$$Q = \mathrm{sgn}\left(\langle i\eta_{2i}\eta_{2i+1} - i\eta_{2i-1}\eta_{2i}\rangle\right) \tag{26}$$

which is odd under lattice translation T_z. We can map this Z_2 bond order to the Ising variable σ^z on the hinge of the HOSPT, and the lattice translation T_z plays a role as the onsite Z_2 symmetry at the HOSPT hinge. As the domain wall of Q carries a Majorana zero mode, the effective theory of such a Majorana chain resembles the hinge of our HOSPT.

For a 1D Majorana chain with an odd number of Majoranas per site and a conserved fermion parity, the LSM theorem predicts the absence of any featureless gapped state. Such a no-go theorem can be extrapolated to the HOSPT hinge, whose low-energy effective theory is either gapless or breaks fermion parity and Z_2 symmetry. In conclusion, the present model seeks a fermionic HOSPT with a gapless hinge protected by Z_2 and subsystem fermion parity.

5. General discussion

In this work, we propose several interaction-enabled higher-order topological phases with subsystem symmetry protection. We identify a series of solvable models that produce gapless hinges or corner states protected by subsystem symmetry and global symmetries. Remarkably, the ungappable nature of the HOSPT hinges can be connected to the 'LSM-type' no-go theorem in lower-dimensional lattice systems, which does not permit a featureless gapped ground state. We employ the flux insertion argument and Wess–Zumino–Witten theory to characterize the anomalous hinge/corner features of these HOSPTs. Several open questions remain, such as a comprehensive mathematical classification of higher-order SPTs, some of which has been partially addressed in [28, 31]. Similarly, the exploration of symmetry-protected topological phases has been extended to other symmetries, such as dipole and quadrupole symmetries [75–77]. Here, we emphasize a few key features of HOSPTs protected by subsystem symmetry.

For SPTs (including higher-order ones) protected by global or spatial symmetries, compactifying one of the spatial dimensions—e.g. reducing a 2d lattice to a thin ladder—causes the boundary modes to vanish due to the interaction between the left and right boundaries, resulting in the cancellation of the boundary anomaly. However, this 'dimensional compactification instability' does not occur in HOSPTs with subsystem symmetry. For instance, compactifying the 2d HOTSC with fermion subsystem symmetry from section 2 into a thin ladder does not annihilate the Majorana corner modes. This is because subsystem fermion parity conservation induces two independent symmetries on each row of the ladder. Similarly, the Majorana zero mode arises from the two-foilated fermion parity conservation intersecting at the corner. Thus, merging two boundaries does not cancel the anomaly generated by subsystem fermion parity.

In our second example in section 3, the HOSPT involves both subsystem and global symmetries, which are intertwined in an anomalous manner on the hinge. If we gauge the global and subsystem symmetries in such a lattice model, it would result in a vector gauge field intertwined with higher-rank gauge potentials, leading to a twisted hybrid fracton theory. It would be interesting to explore whether gauging HOSPTs can generate novel hybrid fracton [78] theories.

Data availability statement

No new data were created or analyzed in this study.

Acknowledgment

This work was initiated at Aspen Center for Physics, which is supported by National Science Foundation Grant PHY-1607611.

References

[1] Fu L 2011 *Phys. Rev. Lett.* **106** 106802
[2] Hsieh T H, Lin H, Liu J, Duan W, Bansil A and Fu L 2012 *Nat. Commun.* **3** 982
[3] Cheng M, Zaletel M, Barkeshli M, Vishwanath A and Bonderson P 2016 *Phys. Rev.* X **6** 041068
[4] Ando Y and Fu L 2015 *Annu. Rev. Condens. Matter Phys.* **6** 361
[5] Slager R-J, Mesaros A, Juričić V and Zaanen J 2013 *Nat. Phys.* **9** 98
[6] Hong S and Fu L 2017 arXiv:1707.02594
[7] Qi Y and Fu L 2015 *Phys. Rev. Lett.* **115** 236801

[8] Huang S-J, Song H, Huang Y-P and Hermele M 2017 *Phys. Rev.* B **96** 205106
[9] Teo J C and Hughes T L 2013 *Phys. Rev. Lett.* **111** 047006
[10] Song H, Huang S-J, Fu L and Hermele M 2017 *Phys. Rev.* X **7** 011020
[11] Watanabe H, Po H C and Vishwanath A 2017 arXiv:1707.01903
[12] Po H C, Vishwanath A and Watanabe H 2017 *Nat. Commun.* **8** 50
[13] Isobe H and Fu L 2015 *Phys. Rev.* B **92** 081304
[14] Benalcazar W A, Bernevig B A and Hughes T L 2017 *Science* **357** 61
[15] Benalcazar W A, Bernevig B A and Hughes T L 2017 *Phys. Rev.* B **96** 245115
[16] Langbehn J, Peng Y, Trifunovic L, von Oppen F and Brouwer P W 2017 *Phys. Rev. Lett.* **119** 246401
[17] Song Z, Fang Z and Fang C 2017 *Phys. Rev. Lett.* **119** 246402
[18] Dwivedi V, Hickey C, Eschmann T and Trebst S 2018 arXiv:1803.08922
[19] Tiwari A, Li M-H, Bernevig B, Neupert T and Parameswaran S 2019 arXiv:1905.11421
[20] You Y and von Oppen F 2018 arXiv:1812.06091
[21] You Y, Devakul T, Burnell F and Neupert T 2018 *Phys. Rev.* B **98** 235102
[22] You Y 2023 *Phys. Rev. Res.* **5** 023201
[23] Peterson C W, Benalcazar W A, Hughes T L and Bahl G 2018 *Nature* **555** 346
[24] Schindler F, Cook A M, Vergniory M G, Wang Z, Parkin S S, Bernevig B A and Neupert T 2018 *Sci. Adv.* **4** eaat0346
[25] Serra-Garcia M, Peri V, Süsstrunk R, Bilal O R, Larsen T, Villanueva L G and Huber S D 2018 *Nature* **555** 342
[26] You Y, Litinski D and von Oppen F 2018 arXiv:1810.10556
[27] Laubscher K, Loss D and Klinovaja J 2019 arXiv:1905.00885
[28] Zhang J-H, Cheng M and Bi Z 2023 *Phys. Rev.* B **108** 045133
[29] Sullivan J, Dua A and Cheng M 2021 *Phys. Rev. Res.* **3** 023123
[30] Zhang H-R, Zhang J-H, Gu Z-C, Zhang R-X and Yang S 2023 *Phys. Rev.* B **108** L060504
[31] May-Mann J, You Y, Hughes T L and Bi Z 2022 *Phys. Rev.* B **105** 245122
[32] Zhang J-H, Ding K, Yang S and Bi Z 2023 *Phys. Rev.* B **108** 155123
[33] You Y, Bibo J and Pollmann F 2020 *Phys. Rev. Res.* **2** 033192
[34] Xu C and Moore J E 2004 *Phys. Rev. Lett.* **93** 047003
[35] You Y, Devakul T, Burnell F and Sondhi S 2018 *Phys. Rev.* B **98** 035112
[36] Devakul T, You Y, Burnell F and Sondhi S 2018 arXiv:1805.04097
[37] Vijay S, Haah J and Fu L 2016 *Phys. Rev.* B **94** 235157
[38] You Y, Devakul T, Burnell F and Sondhi S 2018 arXiv:1805.09800
[39] Devakul T, Williamson D J and You Y 2018 arXiv:1808.05300
[40] Shirley W, Slagle K and Chen X 2018 arXiv:1806.08679
[41] Shirley W, Slagle K and Chen X 2018 arXiv:1806.08625
[42] Shirley W, Slagle K and Chen X 2019 arXiv:1907.09048
[43] Huang S-J, Prem A, Song H and Hermele M 2018 *Bull. Am. Phys. Soc.*
[44] Prem A, Pretko M and Nandkishore R 2017 arXiv:1709.09673
[45] Song H, Prem A, Huang S-J and Martin-Delgado M A 2018 arXiv:1805.06899
[46] You Y, Devakul T, Sondhi S and Burnell F 2019 arXiv:1904.11530
[47] Slagle K, Aasen D and Williamson D 2019 *SciPost Phys.* **6** 043
[48] Williamson D J 2016 *Phys. Rev.* B **94** 155128
[49] Shirley W, Slagle K and Chen X 2019 *SciPost Phys.* **6** 015
[50] He H, You Y and Prem A 2020 *Phys. Rev. B* **101** 165145
[51] Oshikawa M 2000 *Phys. Rev. Lett.* **84** 1535
[52] Hastings M B 2004 *Phys. Rev.* B **69** 104431
[53] Else D V and Thorngren R 2019 arXiv:1907.08204
[54] Jiang S, Cheng M, Qi Y and Lu Y-M 2019 arXiv:1907.08596
[55] Cheng M 2019 *Phys. Rev.* B **99** 075143
[56] Jian C-M, Bi Z and Xu C 2018 *Phys. Rev.* B **97** 054412
[57] Bultinck N and Cheng M 2018 *Phys. Rev.* B **98** 161119
[58] Hsieh T H, Halász G B and Grover T 2016 *Phys. Rev. Lett.* **117** 166802
[59] Thorngren R and Else D V 2018 *Phys. Rev.* X **8** 011040
[60] Fidkowski L and Kitaev A 2010 *Phys. Rev.* B **81** 134509
[61] Fidkowski L and Kitaev A 2011 *Phys. Rev.* B **83** 075103
[62] Benalcazar W A, Li T and Hughes T L 2018 arXiv:1809.02142
[63] Rasmussen A and Lu Y-M 2018 arXiv:1810.12317
[64] Rasmussen A and Lu Y-M 2018 arXiv:1809.07325
[65] Bi Z, You Y-Z and Xu C 2014 *Phys. Rev.* B **90** 081110
[66] Xu C and Senthil T 2013 *Phys. Rev.* B **87** 174412
[67] Levin M and Gu Z-C 2012 *Phys. Rev.* B **86** 115109
[68] Chen X, Wang F, Lu Y-M and Lee D-H 2013 *Nucl. Phys.* B **873** 248
[69] Xu C and Ludwig A W 2013 *Phys. Rev. Lett.* **110** 200405
[70] Else D V and Nayak C 2014 *Phys. Rev.* B **90** 235137
[71] There is a factor since there are two hardcore bosons(spin-1/2) per site.
[72] Bradlyn B, Elcoro L, Vergniory M G, Cano J, Wang Z, Felser C, Aroyo M I and Bernevig B A 2018 *Phys. Rev.* B **97** 035138
[73] Schindler F, Cook A M, Vergniory M G, Wang Z, Parkin S S, Bernevig B A and Neupert T 2017 arXiv:1708.03636
[74] Trifunovic L and Brouwer P 2018 arXiv:1805.02598 [cond-mat.mes-hall]
[75] Lam H T 2024 *Phys. Rev.* B **109** 115142
[76] Lam H T, Han J H and You Y 2024 arXiv:2403.13880
[77] Han J H, Lake E, Lam H T, Verresen R and You Y 2024 *Phys. Rev.* B **109** 125121
[78] Tantivasadakarn N, Ji W and Vijay S 2021 *Phys. Rev.* B **103** 245136